| | |
|---|---|
| ***Publication Year*** | 2018 |
| ***Acceptance in OA@INAF*** | 2020-11-13T10:59:23Z |
| ***Title*** | Bulk Comptonization: new hints from the luminous blazar 4C+25.05 |
| ***Authors*** | Kammoun, E. S.; NARDINI, EMANUELE; Risaliti, G.; GHISELLINI, Gabriele; Behar, E.; et al. |
| ***DOI*** | 10.1093/mnrasl/slx164 |
| ***Handle*** | http://hdl.handle.net/20.500.12386/28309 |
| ***Journal*** | MONTHLY NOTICES OF THE ROYAL ASTRONOMICAL SOCIETY. LETTERS |
| ***Number*** | 473 |

Monthly Notices
of the
ROYAL ASTRONOMICAL SOCIETY

MNRAS **473,** L89–L93 (2018)
Advance Access publication 2017 October 5

doi:10.1093/mnrasl/slx164

# Bulk Comptonization: new hints from the luminous blazar 4C+25.05

E. S. Kammoun,[1]★ E. Nardini,[2] G. Risaliti,[3,2] G. Ghisellini,[4] E. Behar[5] and A. Celotti[1,4,6]

[1]*SISSA, via Bonomea 265, I-34135 Trieste, Italy*
[2]*INAF - Osservatorio Astrofisico di Arcetri, Largo E. Fermi 5, I-50125 Firenze, Italy*
[3]*Dipartimento di Fisica e Astronomia, Università di Firenze, via G. Sansone 1, I-50019 Sesto Fiorentino (Firenze), Italy*
[4]*INAF - Osservatorio Astronomico di Brera, via Bianchi 46, I-23807 Merate, Italy*
[5]*Department of Astronomy, University of Maryland, College Park, MD 20742-2421, USA*
[6]*INFN - Sezione di Trieste, via Valerio 2, I-34127 Trieste, Italy*

Accepted 2017 October 3. Received 2017 October 2; in original form 2017 September 9

## ABSTRACT

Blazars are often characterized by a spectral break at soft X-rays, whose origin is still debated. While most sources show a flattening, some exhibit a blackbody-like soft excess with temperatures of the order of ∼0.1 keV, similar to low-luminosity, non-jetted Seyferts. Here, we present the analysis of the simultaneous *XMM–Newton* and *NuSTAR* observations of the luminous flat-spectrum radio quasar 4C+25.05 ($z = 2.368$). The observed 0.3–30 keV spectrum is best described by the sum of a hard X-ray power law ($\Gamma = 1.38^{+0.05}_{-0.03}$) and a soft component, approximated by a blackbody with $kT_{\rm BB} = 0.66^{+0.05}_{-0.04}$ keV (rest frame). If the spectrum of 4C+25.05 is interpreted in the context of bulk Comptonization by *cold* electrons of broad-line region photons emitted in the direction of the jet, such an unusual temperature implies a bulk Lorentz factor of the jet of $\Gamma_{\rm bulk} \sim 11.7$. Bulk Comptonization is expected to be ubiquitous on physical grounds, yet no clear signature of it has been found so far, possibly due to its transient nature and the lack of high-quality, broad-band X-ray spectra.

**Key words:** galaxies: active – quasars: general – quasars: individual: 4C+25.05 – X-rays: galaxies – X-rays: general.

## 1 INTRODUCTION

According to the unified models of active galactic nuclei (AGNs; Urry & Padovani 1995), radio-loud quasars (RLQs) are characterized by a relativistic jet emitting a collimated non-thermal continuum. If the jet points along the line of sight of the observer, then the quasar is classified as a blazar. The broad-band emission of blazars is characterized by two humps. The first hump (in radio/submillimetre frequencies) is attributed to synchrotron, the second one (in X-/$\gamma$-ray frequencies) to inverse Compton (IC) processes. The seed photons for the IC process can be either intrinsic to the jet, emitted through synchrotron at low frequencies (synchrotron self-Compton, SSC), or originated from the accretion disc and reprocessed by the broad-line region (BLR) and/or the molecular torus (external Compton, EC). The latter is likely the main process in sources revealing a pronounced dominance of the high-frequency hump over the synchrotron one. This usually occurs in the most powerful blazars, i.e. flat-spectrum radio quasars (FSRQs).

The X-ray spectrum of blazars hardens with increasing luminosity. In fact, FSRQs typically show photon indices $\Gamma \sim 1.3$–$1.5$ in the 2–10 keV band (e.g. Wilkes et al. 1992; Boller et al. 2000; de Rosa et al. 2008; Eitan & Behar 2013), which are flatter than usually observed in less luminous RLQs ($\Gamma \sim 1.75$; Sambruna, Eracleous & Mushotzky 1999) or radio-quiet quasars ($\Gamma \sim 1.9$; Piconcelli et al. 2005). Several blazars reveal a flattening in their X-ray spectra at energies below ∼2 keV with respect to a higher energy power law (e.g. Fabian et al. 1998; Piconcelli & Guainazzi 2005), whose origin has been associated with intrinsic cold or warm absorption ($N_{\rm H} \sim 10^{22}$ cm$^{-2}$; e.g. Worsley et al. 2006) or a break of the continuum due to intrinsic curvature of the EC emission from the jet (e.g. Ghisellini et al. 2007; Tavecchio & Ghisellini 2008; Paliya et al. 2016). Some sources, instead, reveal the presence of an excess in emission at similar soft energy ranges. Various scenarios have been suggested in order to explain this feature, such as an excess due to the contribution of the accretion disc emission to the soft X-rays (Sambruna et al. 2006), similar to the one seen in radio-quiet AGNs, or an increase in the contribution of the SSC component (Kataoka et al. 2008). Bulk Comptonization (BC) emission has been proposed as an alternative explanation of spectral flattening and/or excess (e.g. Begelman & Sikora 1987; Sikora, Begelman & Rees 1994; Celotti, Ghisellini & Fabian 2007, hereafter C07). In this context, cold (i.e. non-relativistic) leptons, travelling with a bulk Lorentz factor $\Gamma_{\rm bulk}$, would interact with the photons produced by the accretion disc, and with those reprocessed (re-isotropized) in the BLR and/or scattered by free electrons external to the jet.

★ E-mail: ekammoun@sissa.it

© 2017 The Authors
Published by Oxford University Press on behalf of the Royal Astronomical Society

Downloaded from https://academic.oup.com/mnrasl/article/473/1/L89/4349750 by inaf user on 14 October 2020

The BC emission of disc and BLR photons would result in excess emission with respect to the power-law continuum, emerging, respectively, in the far-ultraviolet (hence not accessible) and mid-X-ray ranges. The latter component would correspond to a hump peaking at ∼3 keV, accompanied by a flattening towards soft energies, which can mimic absorption. The two flavours of the soft X-ray spectral break (deficit or excess) have been usually treated as originated from different processes. C07 modelled the flattening seen in the blazar GB 1428+4217 ($z = 4.72$) assuming a transient BC scenario. The flattening in this source had been ascribed to the presence of intrinsic absorption with column densities $> 10^{22}$ cm$^{-2}$ (e.g. Boller et al. 2000; Fabian et al. 2001; Worsley et al. 2006). BC is expected to be present in all blazars but has never been confirmed, to our knowledge. Besides the case of BG 1428+4217, Kataoka et al. (2008) and de Rosa et al. (2008) presented tentative hints of the presence of BC in the FSRQs PKS 1510−089 ($z = 0.361$) and 4C+04.42 ($z = 0.965$), respectively.

In this letter, we study the X-ray spectrum from a coordinated *XMM–Newton* and *NuSTAR* observation of the FSRQ 4C+25.05 ($z = 2.368$, $\log(M_{\rm BH}/{\rm M}_\odot) = 9.24 \pm 0.44$; Kelly & Bechtold 2007). The following cosmological parameters are assumed: $\Omega_{\rm M} = 0.27$, $\Omega_\Lambda = 0.73$ and $H_0 = 70\,{\rm km\,s^{-1}\,Mpc^{-1}}$.

## 2 OBSERVATIONS AND DATA REDUCTION

4C+25.05 was observed simultaneously by *XMM–Newton* and *NuSTAR*, on 2017 January 15 (Obs. IDs 0790820101 and 60201047002, respectively). The log of the observations is presented in Table 1. We reduced the *XMM–Newton* data using SAS v.15.0.0 and the latest calibration files. We followed the standard procedure for reducing the data of the EPIC-pn (Strüder et al. 2001) and the two EPIC-MOS (Turner et al. 2001) CCD cameras, all operating in full frame mode with a thin filter. The pn and MOS data were processed using `EPPROC` and `EMPROC`, respectively. Source spectra and light curves were extracted from a circular region of a radius of 25 arcsec for both instruments. The corresponding background spectra and light curves were extracted from an off-source circular region located on the same chip, with a radius approximately twice that of the source. We filtered out periods with strong background flares, for a total of around 6 ks. The light curves, background-corrected using `EPICLCCOR`, are shown in Fig. 1 in three different bands (soft, medium and hard). None of them show any significant variability, as they are all well fitted with a constant. Response matrices were produced using the `FTOOLS`, `RMFGEN` and `ARFGEN`. We rebinned the observed 0.3–10 keV spectra using the SAS task `SPECGROUP` to have a minimum S/N of 5 in each energy bin. The MOS1 and MOS2 spectra are consistent, so we combined them using the SAS command `COMBINE`.

The *NuSTAR* data were reduced following the standard pipeline in the *NuSTAR* Data Analysis Software (`NUSTARDAS` v1.6.0), and using the latest calibration files. We cleaned the unfiltered event files with the standard depth correction. We reprocessed the data with the `saamode = optimized` and `tentacle = yes` criteria for a more conservative treatment of the background in proximity of the South Atlantic Anomaly. We extracted the source and background spectra from circular regions of radii 60 and 90 arcsec, respectively, for both focal plane modules (FPMA and FPMB) using the HEASOFT task `NUPRODUCT`, and requiring a minimum S/N of 5 per energy bin. The spectra extracted from both modules are consistent with each other, so they are analysed jointly (but not combined together). Since the background dominates above ∼30 keV, we analysed the *NuSTAR* data in the 3–30 keV observed energy range, corresponding to ∼10–100 keV in the rest frame of the source.

**Table 1.** Net exposure time, average net count rate and ratio of the source to total counts, in the observed 0.3–10 keV band for EPIC-pn and MOS, and 3–30 keV band for FPMA/B.

| Instrument | Net exposure (ks) | Count rate (Count s$^{-1}$) | Source/total |
|---|---|---|---|
| pn | 37.7 | $0.522 \pm 0.003$ | 99 per cent |
| MOS | 49.4 | $0.305 \pm 0.003$ | 98.8 per cent |
| FPMA | 40.4 | $0.047 \pm 0.001$ | 90.3 per cent |
| FPMB | 40.4 | $0.043 \pm 0.001$ | 86.9 per cent |

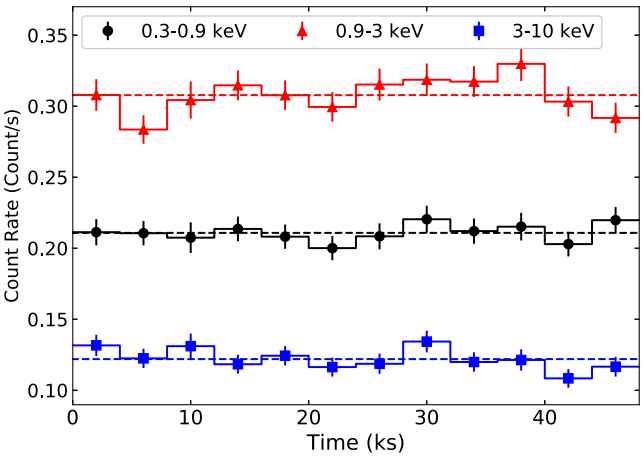


**Figure 1.** *XMM–Newton* light curves (with a time bin of 4 ks) extracted in the 0.3–0.9 keV (black circles), 0.9–3 keV (red triangles) and 3–10 keV (blue squares) observed energy bands, corresponding to the ∼ 1–3, 3–10 and 10–34 keV rest-frame energy bands, respectively. The horizontal dashed lines correspond to the average count rate for each energy band.

## 3 SPECTRAL ANALYSIS

Spectral fitting was performed using XSPEC v12.9s (Arnaud 1996). Unless stated otherwise, uncertainties on the parameters are listed at the 90 per cent confidence level ($\Delta\chi^2 = 2.71$). We included a multiplicative constant, for each instrument, in order to account for the residual uncertainties in the flux calibration between the various detectors, fixing the constant for the EPIC-pn data to unity. The spectra from the various instruments are shown in Fig. 2a.

We started by fitting the hard-energy part of the spectra above 3 keV (observed) with a power-law model with a high-energy cut-off (hereafter PL model), taking into consideration Galactic absorption in the line of sight ($N_{\rm H} = 6.87 \times 10^{20}$ cm$^{-2}$; Kalberla et al. 2005). The fit is statistically acceptable ($\chi^2/{\rm dof} = 181/220$), showing no systematical trend in the residuals, with a photon index $\Gamma = 1.34 \pm 0.13$. We could only set a $3\sigma$ lower limit to the high-energy cut-off of $E_{\rm cut} > 63$ keV (rest frame). The cross-calibration factor between *NuSTAR* and *XMM–Newton* is $f_{\rm NuSTAR} = 1.09 \pm 0.06$, consistent with the values reported by Madsen et al. (2015). The extrapolation of this model to lower energies reveals an excess below ∼5 keV (rest frame), as shown in Fig. 2b. We re-fitted the same model to the full 0.3–30 keV observed range. The fit is statistically acceptable ($\chi^2/{\rm dof} = 373/359$, $p_{\rm null} = 0.29$). The residuals are not statistically significant, yet, qualitatively, they show a subtle overall curvature, leading to a systematic excess in the ∼1.5–3 keV range. The best-fitting photon index is steeper than the previous case ($\Gamma = 1.54 \pm 0.01$). $E_{\rm cut}$ is pegged to its maximum allowed value, with a $3\sigma$ lower limit of 387 keV (rest frame).



Downloaded from https://academic.oup.com/mnrasl/article/473/1/L89/4349750 by inaf user on 14 October 2020

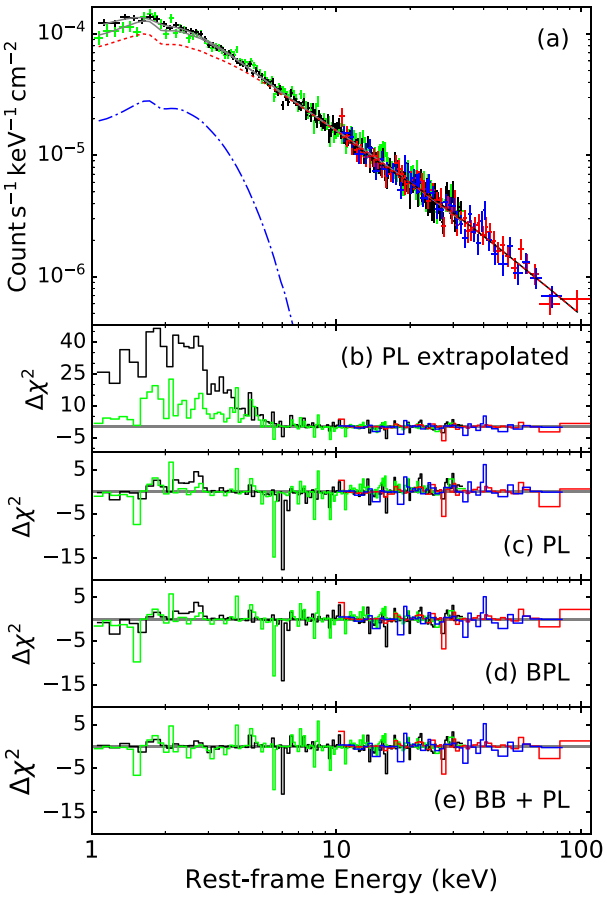


**Figure 2.** Panel (a): spectra from EPIC-pn (black), EPIC MOS (green) and *NuSTAR* FPMA/FPMB (red/blue) plotted together with the total best-fitting model (grey solid line) composed of a PL (red dotted line) and a BB component (blue dash–dotted line). Panel (b): residuals obtained by fitting the spectra above 10 keV (rest frame) with a PL model and then extrapolating it to softer energies, showing an excess in the ∼1–5 keV range. Panels (c–e): residuals obtained by fitting the 1–100 keV range with PL, BPL and BB+PL models, respectively (see Section 3 for details).

The cross-calibration factor between *NuSTAR* and *XMM–Newton* becomes larger, $f_{\rm NuSTAR} = 1.14 \pm 0.04$. We re-fitted the spectra accounting for the possible intrinsic neutral absorption in the rest frame of the source (`zTBabs`; Wilms, Allen & McCray 2000). The fit did not show any improvement ($\chi^2$/dof = 373/358), revealing an intrinsic absorption that is consistent with zero (we could set a $3\sigma$ upper limit on $N_{\rm H}$ to be $9.5 \times 10^{20}$ cm$^{-2}$). We show the residuals corresponding to this model in Fig. 2c.

We considered several models in order to account for the possible excess at soft energies. We first fitted the spectra with a broken power-law model (hereafter BPL model) modified by Galactic absorption only. The fit was statistically acceptable ($\chi^2$/dof = 343/357) with photon indices $\Gamma_{\rm soft} = 1.56 \pm 0.03$ and $\Gamma_{\rm hard} = 1.29 \pm 0.11$. The break and cut-off energies are $E_{\rm b} = 9.2^{+1.2}_{-1.6}$ keV and $E_{\rm cut} = 121^{+139}_{-44}$ keV in the rest frame, respectively. The $3\sigma$ confidence level gives only a lower limit on $E_{\rm cut} > 60$ keV. The cross-calibration factor is $f_{\rm NuSTAR} = 1.08 \pm 0.05$. The fit improves by $\Delta\chi^2 = -30$ for one extra free parameter with respect to the PL model. This improvement is mainly due to the steepening of the spectrum at soft energies, leading to less prominent residual structures (as shown in Fig. 2d), contrary to the commonly seen flattening in other sources (e.g. Piconcelli & Guainazzi 2005).

**Table 2.** Best-fitting parameters obtained by fitting the spectra with the PL, BPL and BB+PL models considered in this analysis. $E_{\rm b}$, $E_{\rm cut}$ and $kT_{\rm BB}$ are reported in the rest frame of the source. The last column represents the peak values of the 1D probability distribution obtained from the MCMC analysis.

| Parameter | PL | BPL | BB+PL | |
|---|---|---|---|---|
| $N_{\rm H}$ ($10^{20}$cm$^{-2}$) | $<9.5^a$ | – | – | – |
| $\Gamma_{\rm soft}$ | – | $1.56 \pm 0.03$ | – | – |
| $E_{\rm b}$ (keV) | – | $9.2^{+1.2}_{-1.6}$ | – | – |
| $\Gamma_{\rm hard}$ | $1.54 \pm 0.01$ | $1.29 \pm 0.11$ | $1.38^{+0.05}_{-0.03}$ | 1.41 |
| $E_{\rm cut}$ (keV) | $>387^a$ | $121^{+139}_{-44}$ | $205^{+256}_{-54}$ | 210 |
| $N_{\rm PL} \times 10^{-4}$ | $3.05 \pm 0.05$ | $3.13 \pm 0.07$ | $2.63^{+0.11}_{-0.08}$ | 2.65 |
| $kT_{\rm BB}$ (keV) | – | – | $0.66^{+0.05}_{-0.04}$ | 0.66 |
| $N_{\rm BB} \times 10^{-5}$ | – | – | $1.92^{+0.32}_{-0.51}$ | 1.8 |
| $\chi^2$/dof | 373/358 | 343/357 | 322/357 | |

*Note.* $^a3\sigma$ lower/upper limit.

We also tested a reflection model (`RELXILL`; Dauser et al. 2013, 2016), even though we do not detect any clear presence of either an iron line or a Compton hump. We fixed the spin to its maximum value (0.998) and we assumed a power-law emissivity profile ($\propto r^{-3}$) with a reflection fraction equal to unity. First, we let the inclination free to vary. The fit resulted in a very high inclination of the disc, which is not physical for this system. Then we fixed the inclination to 5°, which corresponds to a nearly face-on configuration. The fit is statistically acceptable ($\chi^2$/dof = 362/357). The best-fitting photon index, ionization parameter and iron abundance are: $\Gamma = 1.43^{+0.04}_{-0.08}$, $\log\xi = 3.72^{+0.08}_{-0.47}$ and $A_{\rm Fe} = 3.7 \pm 1.2$ solar, respectively. However, this model cannot be considered as a plausible explanation for the spectrum of 4C+25.05. On the one hand, it gives a statistically worse fit compared to the (phenomenological) BPL model. On the other hand, the Doppler-boosted featureless jet emission is expected to be much stronger than any reflection component, thus diluting all other features. Furthermore, it is unlikely in blazars to have a standard (i.e. similar to the non-jetted sources) X-ray corona. If the X-ray source illuminating the disc is a relativistically outflowing corona, then beaming effects would reduce the illumination of the disc, so any reflection component would be negligible (see also King, Lohfink & Kara 2017).

Motivated by the BC model (C07), we considered a model defined as the sum of a blackbody component and a power law (hereafter BB+PL model). The model very well fits the data ($\chi^2$/dof = 322/357), without any systematic residuals. The best-fitting BB+PL model and the corresponding residuals are presented in Fig. 2a,e, respectively. The best-fitting parameters of the BB+PL model, and, for a comparison, of the PL and BPL models as well, are presented in Table 2. The errors on the parameters, for the BB+PL model, are calculated from a Markov chain Monte Carlo (MCMC)[1] analysis, starting from the best-fitting model that we obtained. We used the Goodman–Weare algorithm (Goodman & Weare 2010) with a chain of 500 000 elements (100 walkers and 5000 iterations), discarding the first 75 000 elements as part of the 'burn-in' period. The rest-frame temperature of the blackbody is $kT_{\rm BB} = 0.66^{+0.05}_{-0.04}$ keV, equivalent to a peak energy $E_{\rm peak,\,BB} = 3.93kT_{\rm BB} \simeq 2.6 \pm 0.2$ keV (in $\nu F_\nu$), consistent with the expected value (e.g. C07). In this case, the values of the photon index and the high-energy cut-off are $\Gamma = 1.38^{+0.05}_{-0.03}$ and

[1] We use the XSPEC_EMCEE implementation of the PYTHON EMCEE package for X-ray spectral fitting in XSPEC by Jeremy Sanders (http://github.com/jeremysanders/xspec_emcee).

Downloaded from https://academic.oup.com/mnrasl/article/473/1/L89/4349750 by inaf user on 14 October 2020

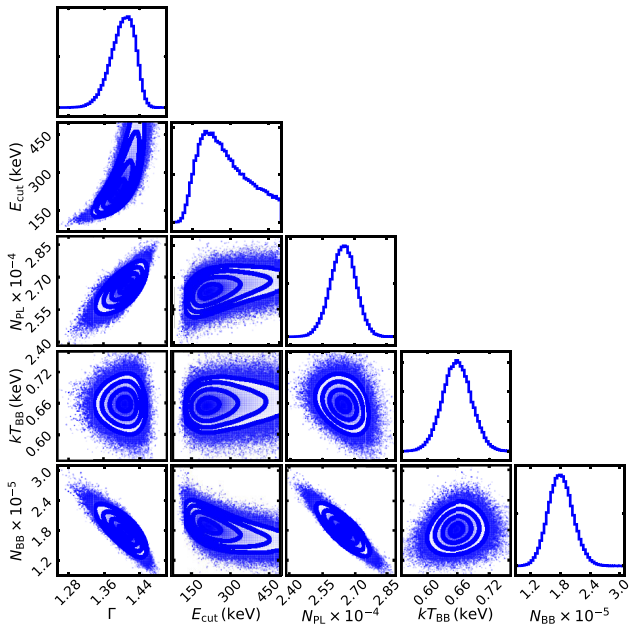


**Figure 3.** Results of the MCMC analysis of the PL+BB model. We show the outputs for photon index Γ, cut-off energy $E_{\rm cut}$ (keV), blackbody temperature $kT_{\rm BB}$ (keV), and normalizations of the power law and the blackbody components $N_{\rm PL}$ and $N_{\rm BB}$, respectively. The 1D histograms show the probability distribution for each parameter normalized to unity.

$E_{\rm cut} = 205^{+256}_{-54}$ keV (rest frame), respectively. These values are consistent with the ones that we obtained by fitting a PL model to the spectra above 3 keV, and the hard component of the BPL model. The $3\sigma$ confidence level gives only a lower limit on $E_{\rm cut} > 110$ keV. The results of the MCMC analysis are shown in Fig. 3. We note that the peak values of the 1D probability distribution obtained from the MCMC analysis (presented in the last column of Table 2) do not exactly coincide with the best-fitting values obtained by minimizing the $\chi^2$ value, but they are consistent within $1\sigma$. The contours show that the temperature of the blackbody is not degenerate with any other parameter, confirming the presence of a significant excess over this energy range. Instead, we found some degeneracy between the normalizations of the PL and that of the BB and between both normalizations and the photon index. The mild degeneracy between the BB normalization with the photon index indicates that a steepening in the PL slope tends to compensate for the BB component. We determine the flux of the source to be $F_{0.3-10} = 2.25^{+0.01}_{-0.05} \times 10^{-12}$ erg s$^{-1}$ cm$^{-2}$ in the 0.3–10 keV observed energy range, which corresponds to a 1–30 keV rest-frame luminosity of $L_{1-30} = (9.44 \pm 0.07) \times 10^{46}$ erg s$^{-1}$. The errors on the flux and luminosity represent the $1\sigma$ confidence level.

## 4 DISCUSSION AND CONCLUSIONS

We have presented the X-ray spectral analysis of the simultaneous *XMM–Newton* and *NuSTAR* observations of the FSRQ 4C+25.05 at $z = 2.368$. The observed spectrum of the source in the 0.3–30 keV range can be well explained by (Table 2):

(i) A simple PL model ($\chi^2$/dof = 373/358) of a photon index $\Gamma = 1.54$. Only upper and lower limits can be set for any intrinsic absorption and high-energy cut-off, respectively.

(ii) A BPL model ($\chi^2$/dof = 343/357), with $\Gamma_{\rm soft} = 1.56$, $\Gamma_{\rm hard} = 1.29$, break energy of $E_{\rm b} = 9.2$ keV and cut-off at $E_{\rm cut} = 121$ keV (rest frame).

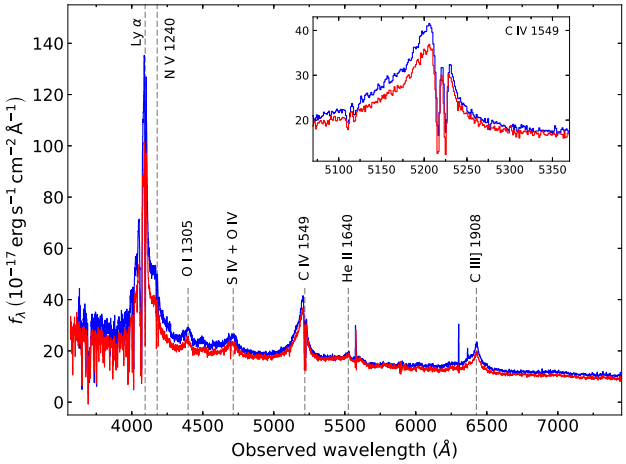


**Figure 4.** Optical spectra of 4C+25.05 obtained from the SDSS-IV. The inset shows the peak of the C IV emission line and the absorption doublet.

(iii) A power-law plus blackbody model ($\chi^2$/dof = 322/357), with $\Gamma = 1.38$, $E_{\rm cut} = 205$ keV and $kT_{\rm BB} = 0.66$ keV.

The BPL model is largely phenomenological, yet the steeper $\Gamma_{\rm soft}$ with respect to $\Gamma_{\rm hard}$ clearly indicates a softening in the soft X-rays, as opposed to the flattening (due to either absorption or intrinsic curvature of the EC emission from the jet) usually observed in high-$z$ blazars. This excess favours the possibility that we are witnessing the spectral signature of BC of BLR photons. Indeed, the BB+PL model has the lowest $\chi^2$ among the various models that we consider in this work. The absence of any absorption in 4C+25.05 is confirmed by the two optical spectra obtained from the Sloan Digital Sky Survey (SDSS-IV; Dawson et al. 2016; Blanton et al. 2017) in 2012 and 2015 (red and blue in Fig. 4, respectively), which do not show any signature of intrinsic cold absorption. We note that the SDSS spectra reveal the presence of narrow 'associated' absorption lines from Ly α, N V, Si IV and C IV (the C IV λλ1548, 1550 doublet is shown in the inset in Fig. 4). These features, rather common in flat-spectrum quasars (e.g. Richards et al. 1999; Richards 2001; Baker et al. 2002), indicate the presence of an ionized low-density ($N_{\rm H\,I} \lesssim 10^{17}$ cm$^{-2}$) absorber close to the central engine. A detailed discussion of these narrow features and of their origin goes beyond the scope of this work. However, we note that this absorption system has been suggested to partially cover the background light (including both the continuum and broad emission-line region) by Barlow & Sargent (1997). We finally point out that the SDSS spectra reveal several broad emission lines, implying the presence of a proper BLR in this source. The BLR component has been already detected and well discussed in previous studies (e.g. Baldwin 1977; Padovani 1989; Kelly & Bechtold 2007).

Our observation time is around 50 ks which corresponds to ∼15 ks or 4 h in the rest frame of the source. As we do not see any variability, this implies that the BC of BLR photons is stable over this time-scale. In fact, C07 showed that the intensity of the BC spectrum from scattered BLR photons increases with time as the jet is accelerating and remains constant once the jet has reached its maximum bulk Lorentz factor. Given $kT_{\rm BB}$, we can estimate the factor $\delta\Gamma_{\rm bulk}$, where $\delta = \Gamma_{\rm bulk}^{-1}(1 - \beta\cos\theta_{\rm V})^{-1}$ is the relativistic Doppler factor and $\theta_{\rm V}$ is the angle between the observer and the jet axis. Following C07, we assume that the BLR emission can be approximated by a blackbody spectrum peaking at the energy of the Ly α, $h\nu_{\rm Ly\,\alpha} = 2.8kT_{\rm BLR} = 13.6$ eV. The observed temperature of the BC component (in the rest frame of the source) is then $kT_{\rm BLR,\,obs} = \delta\Gamma_{\rm bulk}kT_{\rm BLR}$, from which $\delta\Gamma_{\rm bulk} = 136$. One may also



Downloaded from https://academic.oup.com/mnrasl/article/473/1/L89/4349750 by inaf user on 14 October 2020

derive the expressions of $\theta_V$ and the apparent superluminal speed $\beta_a$ as a function of $\Gamma_{bulk}$. For $\Gamma_{bulk} = \delta = 11.7$, we find $\theta_V \simeq 5^\circ$ and $\beta_a \simeq 11.6$. Note that even if BC requires the presence of cold leptons, the jet cannot be pair-dominated since in this case the plasma will suffer strong Compton drag and will be significantly decelerated (Ghisellini & Tavecchio 2010). Alternatively, the jet could be magnetically dominated and proton free, but we consider this possibility unlikely by noting that the SED of this source[2] is very similar to that of a typical FSRQ, for which Celotti & Ghisellini (2008) model the high-energy spectrum as IC emission. The X-ray spectrum of FSRQ 4C+25.05 is rising (in $\nu F_\nu$) to higher energy, and the luminosity is already similar to that in the synchrotron component. If the X-rays are due to IC scattering, the Compton peak dominates the bolometric output, and the magnetic-field component can only marginally contribute to the jet energy density.

BC emission is expected to be present in the X-ray spectra of all blazars. However, it has not been clearly detected until now. This can be mainly due to the presence of strong SSC and EC emission diluting any other emission features. In powerful FSRQs, the SSC is relatively weak, and the EC spectrum is exceptionally hard. These sources could be therefore the best candidates to search for BC signatures. Excesses similar to the one that we have found at soft energies have been reported is several blazars at $z < 1$ (e.g. Piconcelli et al. 2005; Sambruna et al. 2006; de Rosa et al. 2008; Kataoka et al. 2008), and modelled with a blackbody component with $kT_{BB} \sim 0.1$–$0.2$ keV. However, this temperature range is lower than expected for the BC process, leading to low values of $\Gamma_{bulk} \sim 5$–$6$. This makes 4C+25.05 an exceptional source where a softening in the X-ray spectrum has been detected for the first time, to our knowledge, above $z = 1$, contrary to the soft X-ray flattening that has been observed up to $z = 4.72$ (e.g. Worsley et al. 2006). In our case, the hard X-ray photon index obtained by applying a BB+PL model is only slightly flatter than the one obtained by fitting a simple PL ($\Delta\Gamma \sim 0.15$). This difference would be negligible for a low S/N at high energies. The failure in detecting BC, in the past, could be due to the possible overestimate of the slope of the hard X-ray continuum. Our results show that simultaneous *XMM–Newton* and *NuSTAR* observations, providing high S/N spectra over the observed 0.3–30 keV band, are capable of revealing the presence of the elusive BC feature at soft energies. We finally note that BC is expected to be a transient feature. Hence, a further and longer monitoring of the source, catching it probably in other spectral states, would be needed in order to confirm this scenario. Moreover, it could be worth revisiting the model of BC effects, based on more general assumptions and geometries, including a disc-like structure for the BLR (similar to the one observed in a radio-quiet AGN) instead of the semispherical shell geometry considered by C07.

## ACKNOWLEDGEMENTS

EN is supported by the EU through the Horizon 2020 Marie Skłodowska-Curie grant agreement no. 664931. EB is supported by the EU through the Horizon 2020 Marie Skłodowska-Curie grant agreement no. 655324. The results presented in this letter are based on data obtained with the *NuSTAR* mission, a project led by the California Institute of Technology, managed by the Jet Propulsion Laboratory, and funded by NASA; *XMM–Newton*, an ESA science mission with instruments and contributions directly funded by ESA member states and NASA. This research has made use of the NuSTAR Data Analysis Software (NuSTARDAS), jointly developed by the ASI Science Data Center (Italy) and the California Institute of Technology (USA). The figures were generated using `matplotlib` (Hunter 2007), a PYTHON library for publication of quality graphics. The MCMC results were presented using the open source code `corner.py` (Foreman-Mackey 2016).

[2] The SED including all archival data can be built using the tool at https://tools.asdc.asi.it/.

## REFERENCES

Arnaud K. A., 1996, in Jacoby G. H., Barnes J., eds, ASP Conf. Ser. Vol. 101, Astronomical Data Analysis Software and Systems V. Astron. Soc. Pac., San Francisco, p. 17
Baker J. C., Hunstead R. W., Athreya R. M., Barthel P. D., de Silva E., Lehnert M. D., Saunders R. D. E., 2002, ApJ, 568, 592
Baldwin J. A., 1977, ApJ, 214, 679
Barlow T. A., Sargent W. L. W., 1997, AJ, 113, 136
Begelman M. C., Sikora M., 1987, ApJ, 322, 650
Blanton M. R. et al., 2017, AJ, 154, 28
Boller T., Fabian A. C., Brandt W. N., Freyberg M. J., 2000, MNRAS, 315, L23
Celotti A., Ghisellini G., 2008, MNRAS, 385, 283
Celotti A., Ghisellini G., Fabian A. C., 2007, MNRAS, 375, 417 (C07)
Dauser T., Garcia J., Wilms J., Böck M., Brenneman L. W., Falanga M., Fukumura K., Reynolds C. S., 2013, MNRAS, 430, 1694
Dauser T., García J., Walton D. J., Eikmann W., Kallman T., McClintock J., Wilms J., 2016, A&A, 590, A76
Dawson K. S. et al., 2016, AJ, 151, 44
de Rosa A., Bassani L., Ubertini P., Malizia A., Dean A. J., 2008, MNRAS, 388, L54
Eitan A., Behar E., 2013, ApJ, 774, 29
Fabian A. C., Iwasawa K., McMahon R. G., Celotti A., Brandt W. N., Hook M., 1998, MNRAS, 295, L25
Fabian A. C., Celotti A., Iwasawa K., Ghisellini G., 2001, MNRAS, 324, 628
Foreman-Mackey D., 2016, J. Open Source Softw., 1, 24
Ghisellini G., Tavecchio F., 2010, MNRAS, 409, L79
Ghisellini G., Foschini L., Tavecchio F., Pian E., 2007, MNRAS, 382, L82
Goodman J., Weare J., 2010, Comm. App. Math. Comput. Sci., 5, 65
Hunter J. D., 2007, Comput. Sci. Eng., 9, 90
Kalberla P. M. W., Burton W. B., Hartmann D., Arnal E. M., Bajaja E., Morras R., Pöppel W. G. L., 2005, A&A, 440, 775
Kataoka J. et al., 2008, ApJ, 672, 787
Kelly B. C., Bechtold J., 2007, ApJS, 168, 1
King A. L., Lohfink A., Kara E., 2017, ApJ, 835, 226
Madsen K. K. et al., 2015, ApJS, 220, 8
Padovani P., 1989, A&A, 209, 27
Paliya V. S., Parker M. L., Fabian A. C., Stalin C. S., 2016, ApJ, 825, 74
Piconcelli E., Guainazzi M., 2005, A&A, 442, L53
Piconcelli E., Jimenez-Bailón E., Guainazzi M., Schartel N., Rodríguez-Pascual P. M., Santos-Lleó M., 2005, A&A, 432, 15
Richards G. T., 2001, ApJS, 133, 53
Richards G. T., York D. G., Yanny B., Kollgaard R. I., Laurent-Muehleisen S. A., Vanden Berk D. E., 1999, ApJ, 513, 576
Sambruna R. M., Eracleous M., Mushotzky R. F., 1999, ApJ, 526, 60
Sambruna R. M., Gliozzi M., Tavecchio F., Maraschi L., Foschini L., 2006, ApJ, 652, 146
Sikora M., Begelman M. C., Rees M. J., 1994, ApJ, 421, 153
Strüder L. et al., 2001, A&A, 365, L18
Tavecchio F., Ghisellini G., 2008, MNRAS, 386, 945
Turner M. J. L. et al., 2001, A&A, 365, L27
Urry C. M., Padovani P., 1995, PASP, 107, 803
Wilkes B. J., Elvis M., Fiore F., McDowell J. C., Tananbaum H., Lawrence A., 1992, ApJ, 393, L1
Wilms J., Allen A., McCray R., 2000, ApJ, 542, 914
Worsley M. A., Fabian A. C., Pooley G. G., Chandler C. J., 2006, MNRAS, 368, 844

This paper has been typeset from a TEX/LATEX file prepared by the author.

Downloaded from https://academic.oup.com/mnrasl/article/473/1/L89/4349750 by inaf user on 14 October 2020